# Direct observation of the dispersion and relaxation of photoexcited electrons in InAs

Junpei Azuma, Kazutoshi Takahashi, and Masao Kamada
*Synchrotron Light Application Center, Saga University, 1 Honjo, Saga 840-8502, Japan*
(Received 14 October 2009; revised manuscript received 24 February 2010; published 30 March 2010)

Time- and angle-resolved photoemission spectroscopy has been applied to the excited state in *n*-type InAs. The electrons populated by the direct optical transition were clearly observed in the middle of the conduction band. The relaxation of the photoexcited electrons was also observed along the dispersion of the lowest conduction band on the $\Sigma$ line. The nonequilibrium electron distribution on the relaxation was found within 1 ps.

DOI: 10.1103/PhysRevB.81.113203 PACS number(s): 72.20.Jv, 71.20.Nr, 71.35.−y

Angle-resolved photoemission spectroscopy (ARPES) is a powerful tool to investigate the dispersion relation of occupied electronic states. With the incredible advances of the electron energy analyzer and the excitation light source, occupied electronic states can be easily understood with a good energy resolution of less than 10 meV.[1,2]

On the other hand, it is not easy to know the dispersion relation of unoccupied states and the excited electron dynamics. For example, an inverse photoemission spectroscopy (IPES) is a well-known technique to study unoccupied electronic states but the IPES has the difficulty that the cross section of the inverse photoemission process is $10^5$ times smaller than that of the photoemission process.[3]

Two-photon photoemission (2PPE) technique has been developed with the progress of laser technology in order to investigate unoccupied electronic states, and the pioneer works on 2PPE have been reported.[4–6] It is expected that the combination of the ultrafast laser technology and ARPES, which have evolved dramatically over the last decade, will be a breakthrough of the electron spectroscopy for unoccupied electronic states.

InAs is one of interesting and useful materials for terahertz (THz) emission. It was reported that the ultrafast excited electron transport driven by the intrinsic surface electric field or the gradient of the photoexcited charges generates ultrashort electromagnetic wave packets called as the THz emission, when ultrafast laser pulses are incident on semiconductor surfaces. It has been reported that the THz intensity of InAs is one order of magnitude higher than those of InP and GaAs.[7] Liu *et al.* observed the THz emission from various InAs wafers and simulated with the drift-diffusion equation.[8] In their calculation, the electron temperature was assumed to be constant at 6000 K in 1 ps, even though their model of the electron transport was governed by the diffusion constant $D=k_BT_e\mu/e$. Nansei *et al.* reported the temporal evolution of the hot luminescence, i.e., the luminescence from the excited carriers on the relaxation, in InAs with the 1.6 eV excitation by using the up-conversion technique.[9] Since it is difficult to calibrate the spectral intensity obtained by the upconversion, they also assumed the initial electron temperature $T_e$ of 6000 K and that it would decay exponentially at 2.3 ps lifetime in order to interpret the temporal behavior of the hot luminescence. The electron dynamics in the early stage of the photoexcitation in InAs have not been clarified yet. In the present report, the time- and angle-resolved photoemission spectroscopy (hereafter abbreviated as TARPS) for the two-photon photoemission has been applied to investigate the dispersion and relaxation of the photoexcited states in InAs.

The schematic drawing of the TARPS system was shown in the previous reports.[10,11] A femtosecond laser system and a high-resolution angle-resolved photoemission spectrometer were combined in the present system. The laser system was Ti:sapphire regenerative amplifier (Coherent RegA9000) with the Ti:sapphire oscillator (Coherent Mira900F). This laser can generate the intense laser pulses with the duration of less than 200 fs at the high repetition rate from 10 to 300 kHz. The fundamental of $h\nu=1.55$ eV was used as a pump beam and the third harmonics was generated as a probe beam by the nonlinear optical crystal of $\beta$-barium borate. The time resolution of the present system was obtained as 360 fs by measuring cross correlation of the pump and probe pulses. The powers of the pump and probe lasers were limited to avoid the spectral distortion due to the space-charge effect. The actual conditions of the repetition rate, pump, and probe powers were 300 kHz, 15 $MW/cm^2$, and 1.5 $MW/cm^2$, respectively.

The photoemission spectrometer consisted of the hemispherical electron energy analyzer of a 200 mm inner radius equipped with a charge-coupled device (CCD) camera together with a microchannel plate (MCP) (MB Scientific A-1). The total-energy resolution of the experimental apparatus was determined as 45 meV by the two-photon photoemission spectra of a Au Fermi level. The angle resolutions of the electron energy analyzer and the present TARPS measurement were 10 mrad and 44 mrad, respectively, the latter of which was determined by the step of sample rotation. The system was constructed at the Saga University beamline BL13 in the SAGA Light Source (SAGA-LS).[12,13] It should be emphasized that the TARPS and the conventional x-ray photoemission spectroscopy (XPS) measurements have been performed to one and the same sample at the machine time.

The sample used in the present experiment was the *n*-type InAs(001) wafer with the carrier concentration of $1.4\times10^{17}$–$1.7\times10^{17}$ $cm^{-3}$ (GIRMET Ltd.). The clean surface of InAs(001) was obtained by the ion bombardment and annealing (IBA) as reported in Ref. 14. Ne gas was used in the ion bombardment with the ion energy of 1 kV and the incident angle of 45° because the Ne sputtering yield is smaller than that of Ar. The annealing temperature was 600 K for the ion bombardment. The final annealing was performed at 750 K for 15 min. After the IBA procedure, a good $c(8\times2)$ pat-

 

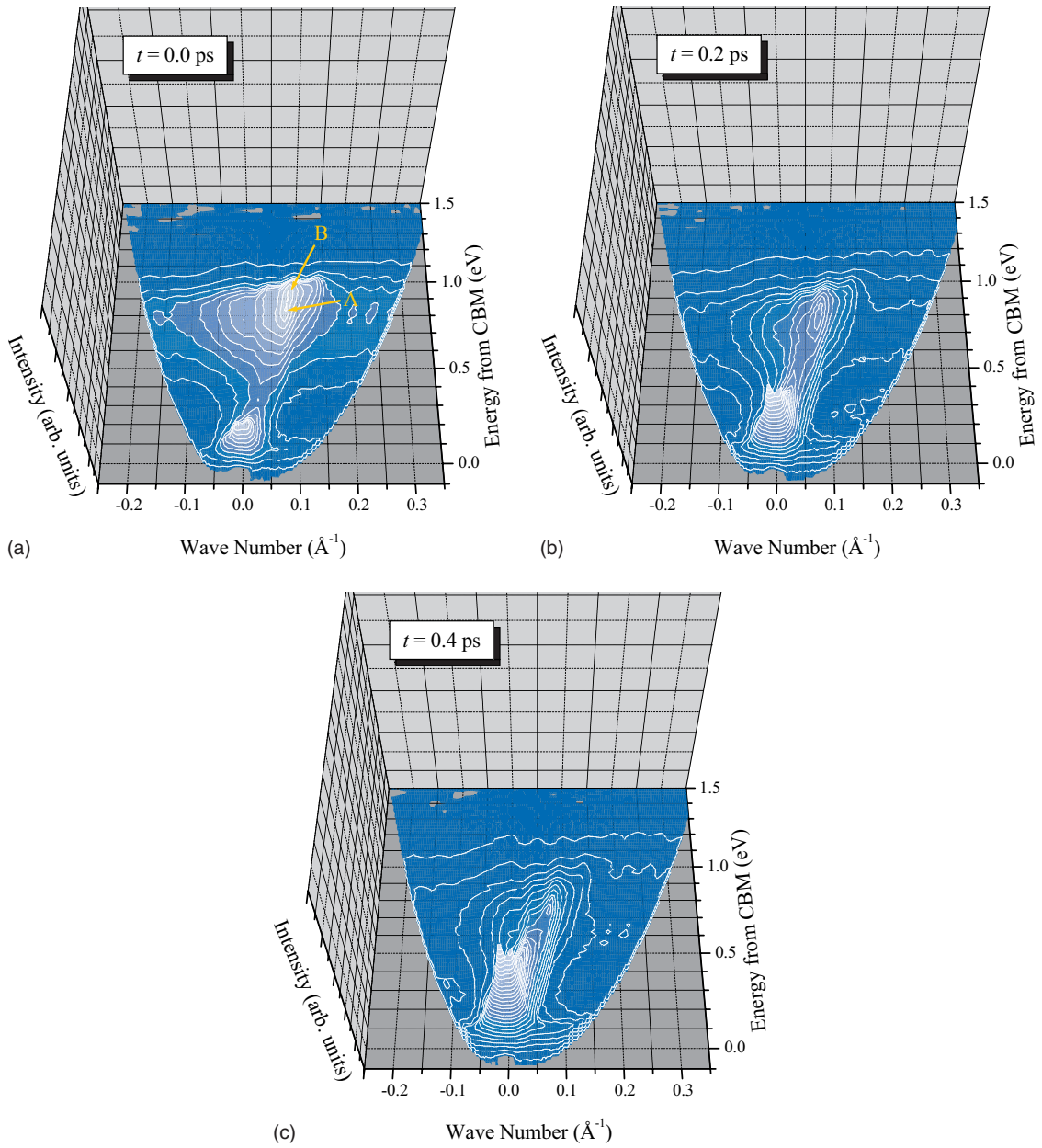


FIG. 1. (Color) Bird views of TARPS for the photoexcited electrons in the *n*-type InAs with the delay time of 0.0 (top left), 0.2 (top right), and 0.4 ps (bottom left). Arrows show two electron peaks (see text).

tern was obtained by the low-energy electron diffraction measurement. Previously it was reported that the carrier concentration on the InAs surface was increased up to $10^{19}$ $cm^{-3}$ order by the electronic damage caused by the IBA treatment with Ar.[15] Thus, there is a possibility that the Fermi level of the surface region could be moved by the change in the carrier concentration but the shift of the Fermi-level pinning was not clearly observed in our experimental conditions.

The base pressures of the photoemission spectrometer and the preparation chamber were less than $1.0\times10^{-7}$ Pa. Little contaminations of carbon and oxygen were observed on the IBA-treated InAs surface by the XPS measurement before and after the TARPS experiment.

Figure 1 shows the bird views of TARPS in the *n*-type InAs. The abscissas show the momentum $k_{\parallel}$ parallel to the [110] direction and the ordinates indicate the energy from the conduction-band minimum (CBM), which was determined by the Fermi level of the metal sample holder and the dopant dependence of the Fermi level in InAs.[16] The photoemission intensities are represented by the heights. The ridge related to the band dispersion of the excited state can be seen clearly in the bird views. At the delay time of 0.0 ps, additional electron peaks are observed at $(k_{\parallel},E)=(0.07,0.6)$ and (0.08, 0.7) along the ridge, as shown by the arrows in Fig. 1. As discussed later about the time dependence of the excited electron distribution, the intensities of the peaks decrease but still remain up to the 0.7 ps time delay. This means that the electron peaks are attributed to the real excitation in the excited states but not to the two-photon excitation of the occupied

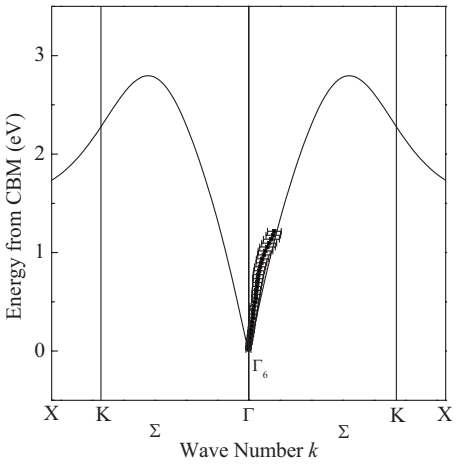


FIG. 2. Peaks obtained by the Gaussian fittings for the MDCs, which were averaged from 0.0 to 1.0 ps delay time in the *n*-type InAs. The solid line indicates the theoretical conduction-band dispersion (see text).

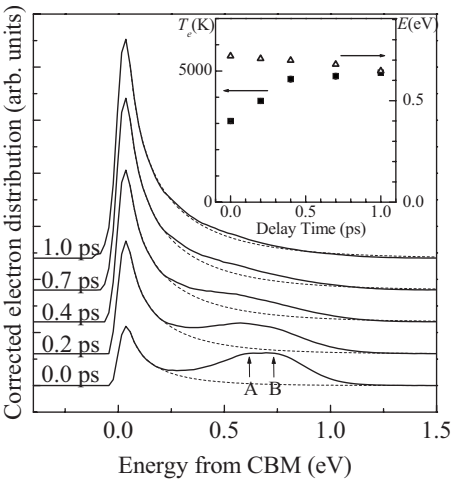


FIG. 3. Time dependence of the photoexcited electron distributions in the *n*-type InAs. The solid lines indicate the electron distributions in the Σ-*E* plane obtained from the TARPS results. Arrows show two electron peaks. The dashed lines are the fitting results of the quasiequilibrated electron distributions (see text). The inset shows the time dependence of the excited electron temperature (closed square) and the average excess energy of the nonequilibrium distribution (open triangle).

valence states. It is also clearly seen that the relaxed electrons are accumulated in the lower-energy region of the band bottom and their intensity increases as the time goes by.

The square dots in Fig. 2 show the peaks obtained from the momentum distribution curves (MDCs), which were averaged from 0.0 to 1.0 ps delay time since the excited electron distributions are localized in *k*-*E* space at some delay times. One can clearly see the dispersion of the excited state, which can be seen as the ridge in the bird views of TARPS. The band structures in the InAs bulk were previously reported by the nonlocal pseudopotential calculations.[17,18] These theoretical bands were modified empirically to reproduce the experimentally determined band dispersion data of the III-V semiconductors along the Σ line, which were obtained from the normal-emission ARPES spectra on the (110) surface by changing the excitation photon energy.[18] From these results, the energy difference between the $\Gamma_8$ point of the valence-band maximum (VBM) and the $\Gamma_7$ and the $\Gamma_8$ points of the upper conduction band is 4.4–5.2 eV and becomes smaller as the wave number $k$ increases. It was also reported by the inverse photoemission study that the peak due to $\Gamma_7$ and $\Gamma_8$ points of the upper conduction band was found above 4.5 eV from the VBM with the bandwidth of about 2 eV.[19] Therefore, the photoemission from the lowest conduction band should occur near by the $\Gamma_6$ point, i.e., CBM, to $\Gamma_7$ and $\Gamma_8$ points of the upper conduction band with the 4.65 eV excitation. In other words, the $k_\perp$ of the final state is considered to be small and the photoemission should reflect the conduction-band dispersion on the Σ line approximately when the excited electrons in the lowest conduction band are reexcited by the 4.65 eV probe. In Fig. 2, the theoretical conduction-band dispersion from Ref. 18 is shown by the solid line. It can be seen that the theoretical band structure fits well to the experimental result. Therefore, the observed excited-state dispersion can be assigned as the lowest InAs bulk conduction band along the Σ line. The two observed peaks of the photoemission at the 0.0 ps delay time can be explained as the electrons populated with the direct optical transition from the light- and heavy-hole bands since the energy splitting of the light- and heavy-hole bands around $k=0.08$ Å$^{-1}$ on the Σ line can be read as about 100 meV from the same calculation.

The energy distributions of the photoexcited electrons in the Σ-*E* plane from 0.0 to 1.0 ps are shown in Fig. 3. The abscissa shows the energy measured from the conduction-band minimum. The solid lines indicate the experimentally obtained electron distributions. The broad excited electron band is clearly observed around 0.7 eV from 0.0 to 0.4 ps, which is the composite band with the different electron peaks and corresponds to the electrons populated by the direct optical transition in the conduction band, as mentioned before. It can be seen that the band of the directly populated nonequilibrium electrons shifts to the lower-energy side with the intensity decreased as the delay time increases. After the band almost disappears in 1.0 ps, the tail structure of the quasiequilibrium electrons remains. The quasiequilibrated electron distribution can be fitted by the following equation:

$$N(E) \propto E^{-1/2} \exp(-E/k_B T_e), \tag{1}$$

where $T_e$ is the electron temperature and $E^{-1/2}$ represents the density of states in the one-dimensional parabolic band. The dashed lines show the fitting result of Eq. (1). The electron distribution can be separated into the equilibrium and nonequilibrium parts. The closed squares in the inset show the obtained electron temperatures from 0.0 to 1.0 ps. The averaged excess energies of the nonequilibrium electrons are also shown by the open triangle. At the zero delay time, the equilibrium electron energy obtained from $T_e$ is about half of the excess energy of the directly populated nonequilibrium electrons. The electron temperature of the quasiequilibrium electrons is raised over time by taking the heat, in other words the excess energy, from the nonequilibrated electrons. The

averaged electron energies of the equilibrated and nonequilibrated parts achieve almost balanced at the 1.0 ps delay time.

Generally, the energy relaxation of photoexcited electrons is governed by the electron-electron and electron-phonon interactions. Ichibayashi *et al.* reported that the averaged electron energy at 100 fs delay time in Si is less than half of the excess energy given by the photoexcitation, indicating that more than half of the electron excess energy is transferred to the lattice within 100 fs during the intravalley scattering.[20] This means that the *e-p* scattering is dominant process of the energy relaxation in Si. On the contrary, 90% of the electron excess energy still remains at 1.0 ps delay time in InAs. It indicates that the *e-p* interaction has the secondary role in the energy relaxation in InAs, which originates the decay of $T_e$ with a few picosecond lifetime as reported by Nansei *et al.*[9] The energy relaxation of the early stage in InAs is dominated by the electron-electron interaction as one can see in the balancing of the equilibrated and nonequilibrated parts of the excited electrons. However, it is difficult to explain the cold electron distribution at the zero delay time with the half of the excess energy only by assuming the energy transfer among the photoexcited electrons because the total and also the averaged electron energies in the excited states are conserved in that process. In order to explain the cold electron distribution, it is necessary to consider the impact ionization, which is due to the electron-electron interaction between the conduction and the valence electrons.[21] Since the directly populated electrons in the middle of the conduction band can interact to little amount of the excited electrons and also a large number of valence electrons in the initial stage of the photoexcitation, one excited electron can easily lose the excess energy by exciting another valence electron to the conduction band. This is the reason why the initial temperature of the quasiequilibrium electrons is almost half as much as that expected from the excess energy of the photoexcitation. As the photoexcited electrons increase, the quasiequilibration among the excited electrons takes the place of the impact ionization of the valence electrons by the screening.

In summary, it is concluded from the TARPS measurement that the conduction-band dispersion and the photoexcited electron relaxation in the InAs were directly observed. The wavelength tunable TARPS measurement will be especially useful to measure the three-dimensional dispersion of the bulk unoccupied electronic states.

Authors are grateful to Hangyo, Nagashima in the Institute of Laser Engineering, Osaka University, and Tani in Research Center for Development of Far-Infrared Region, University of Fukui for providing the sample wafer. This work was partially supported by the "Kyushu-area Nanotechnology Network Project" of the Ministry of Education, Culture, Sports, Science and Technology.

[1] S. Hüfner, *Photoelectron Spectroscopy*, 2nd ed. (Springer, Berlin, 1996).
[2] S. Hüfner, *Very High Resolution Photoelectron Spectroscopy* (Springer, Berlin, 2007).
[3] N. V. Smith, Rep. Prog. Phys. **51**, 1227 (1988).
[4] C. A. Schmuttenmaer, C. Cameron Miller, J. W. Herman, J. Cao, D. A. Mantell, Y. Gao, and R. J. D. Miller, Chem. Phys. **205**, 91 (1996).
[5] H. Petek and S. Ogawa, Prog. Surf. Sci. **56**, 239 (1997).
[6] P. Szymanski, S. Garrett-Roe, and C. B. Harris, Prog. Surf. Sci. **78**, 1 (2005).
[7] N. Sarukura, H. Ohtake, S. Izumida, and Z. Liu, J. Appl. Phys. **84**, 654 (1998).
[8] K. Liu, J. Xu, T. Yuan, and X.-C. Zhang, Phys. Rev. B **73**, 155330 (2006).
[9] H. Nansei, S. Tomimoto, S. Saito, and T. Suemoto, Phys. Rev. B **59**, 8015 (1999).
[10] S. Tokudomi, J. Azuma, K. Takahashi, and M. Kamada, J. Phys. Soc. Jpn. **77**, 014711 (2008).
[11] J. Azuma, S. Tokudomi, K. Takahashi, and M. Kamada, Phys. Status Solidi C **6**, 307 (2009).
[12] K. Takahashi, Y. Kondo, J. Azuma, and M. Kamada, J. Electron Spectrosc. Relat. Phenom. **144-147**, 1093 (2005).
[13] K. Takahashi, J. Azuma, S. Tokudomi, and M. Kamada, *Synchrotron Radiation Instrumentation: Ninth International Conference on Synchrotron Radiation Instrumentation*, AIP Conf. Proc. No. 879 (AIP, New York, 2007), p. 1218.
[14] I. Aureli, V. Corradini, C. Miriani, E. Placidi, F. Arciprete, and A. Balzarotti, Surf. Sci. **576**, 123 (2005).
[15] G. R. Bell, C. F. McConville, and T. S. Jones, Appl. Surf. Sci. **104-105**, 17 (1996).
[16] M. Levinshtein, S. Rumyantsev, and M. Shur, *Handbook on Semiconductor Parameters* (World Scientific, Singapore, 1996), Vol. 1.
[17] J. R. Chelikowsky and M. L. Cohen, Phys. Rev. B **14**, 556 (1976).
[18] G. P. Williams, F. Cerrina, G. J. Lapeyre, J. R. Anderson, R. J. Smith, and J. Hermanson, Phys. Rev. B **34**, 5548 (1986).
[19] W. Drube, D. Straub, and F. J. Himpsel, Phys. Rev. B **35**, 5563 (1987).
[20] T. Ichibayashi and K. Tanimura, Phys. Rev. Lett. **102**, 087403 (2009).
[21] B. K. Ridley, *Quantum Processes in Semiconductors*, 4th ed. (Oxford University Press, Oxford, 1999).